Aging Cell (2008) **7**, pp89–100 Doi: 10.1111/j.1474-9726.2007.00354.x

Delayed kinetics of DNA double-strand break processing in normal and pathological aging

Olga A. Sedelnikova,[1] Izumi Horikawa,[2,4] Christophe Redon,[1] Asako Nakamura,[1] Drazen B. Zimonjic,[3] Nicholas C. Popescu[3] and William M. Bonner[1]

[1]Laboratory of Molecular Pharmacology, [2]Laboratory of Biosystems and Cancer, [3]Laboratory of Experimental Carcinogenesis, and [4]present address: Laboratory of Human Carcinogenesis, Center for Cancer Research, National Cancer Institute, National Institutes of Health, Bethesda, MD, 20892, USA

Summary

Accumulation of DNA damage may play an essential role in both cellular senescence and organismal aging. The ability of cells to sense and repair DNA damage declines with age. However, the underlying molecular mechanism for this age-dependent decline is still elusive. To understand quantitative and qualitative changes in the DNA damage response during human aging, DNA damage-induced foci of phosphorylated histone H2AX (γ-H2AX), which occurs specifically at sites of DNA double-strand breaks (DSBs) and eroded telomeres, were examined in human young and senescing fibroblasts, and in lymphocytes of peripheral blood. Here, we show that the incidence of endogenous γ-H2AX foci increases with age. Fibroblasts taken from patients with Werner syndrome, a disorder associated with premature aging, genomic instability and increased incidence of cancer, exhibited considerably higher incidence of γ-H2AX foci than those taken from normal donors of comparable age. Further increases in γ-H2AX focal incidence occurred in culture as both normal and Werner syndrome fibroblasts progressed toward senescence. The rates of recruitment of DSB repair proteins to γ-H2AX foci correlated inversely with age for both normal and Werner syndrome donors, perhaps due in part to the slower growth of γ-H2AX foci in older donors. Because genomic stability may depend on the efficient processing of DSBs, and hence the rapid formation of γ-H2AX foci and the rapid accumulation of DSB repair proteins on these foci at sites of nascent DSBs, our findings suggest that decreasing efficiency in these processes may contribute to genome instability associated with normal and pathological aging.

Key words: aging; cellular senescence; DNA damage; DSB repair; γ-H2AX; Werner syndrome.

Introduction

A growing body of evidence indicates that cellular response to DNA damage plays a key role in the regulation of aging in multicellular organisms (Hasty & Vijg, 2002; Collado *et al*., 2007). Telomere dysfunction at the end of cellular replicative life span is recognized as DNA damage and triggers a permanent cell cycle arrest called replicative senescence (Stewart & Weinberg, 2006). Acute cellular stresses, such as oxidative damage by reactive oxygen species (Colavitti & Finkel, 2005) and oncogene activation (Bartkova *et al*., 2006; Di Micco *et al*., 2006), also induce DNA damage signaling, which may lead to a checkpoint response called stress-induced premature senescence. Cellular senescence, induced by DNA damage signaling either replicatively or prematurely, is thought to affect tissue homeostasis and functions, and therefore organismal life span (Campisi, 2005; Zhang, 2007).

Transgenic mice deficient in DNA repair proteins exhibit premature senescence in embryonic fibroblasts and an early onset of aging-specific changes *in vivo* (Celeste *et al*., 2002; De Boer *et al*., 2002; Hasty *et al*., 2003). In humans, many premature aging syndromes are caused by mutations in genes encoding proteins involved in DNA repair, such as the family of RecQ-like DNA helicases (Hickson, 2003; Karanjawala & Lieber, 2004; Dhillon *et al*., 2007). Among these disorders is Werner syndrome (WS), which is characterized by a shortened life span, an early onset of aging-associated symptoms (Bohr, 2005; Kyng & Bohr, 2005) and an increased incidence of cancers (Nehlin *et al*., 2000; Shen & Loeb, 2001; Ostler *et al*., 2002). Another premature aging syndrome, Hutchinson–Gilford progeria (Mattout *et al*., 2006), is caused by mutations in the *LMNA* gene and is also associated with an activation of DNA damage responses (Liu *et al*., 2006). Because of many features shared by accelerated aging in patients with these disorders and physiological aging in normal individuals (Kipling *et al*., 2004; Scaffidi & Misteli, 2006), they are thought to be a good model for studying aging in humans (Cheng *et al*., 2007).

DNA double-strand breaks (DSBs) accumulate during both *in vivo* aging and *in vitro* cellular aging in culture. A modest but significant increase in DSBs was detected in aged mice by microgel electrophoresis (Singh *et al*., 2001). We and others demonstrated that the DSB-specific foci, which contain phosphorylated histone H2AX (γ-H2AX), 53BP1, Mre11, Rad50 and Nbs1

Correspondence
Dr Olga Sedelnikova, Laboratory of Molecular Pharmacology, Center for Cancer Research, National Cancer Institute, National Institutes of Health, Bldg. 37, Room 5050, 9000 Rockville Pike, Bethesda, MD, 20892, USA. Tel.: 1-301-402-3649; fax: 1-301-402-0752; e-mail: sedelnio@mail.nih.gov

Accepted for publication 7 *November* 2007

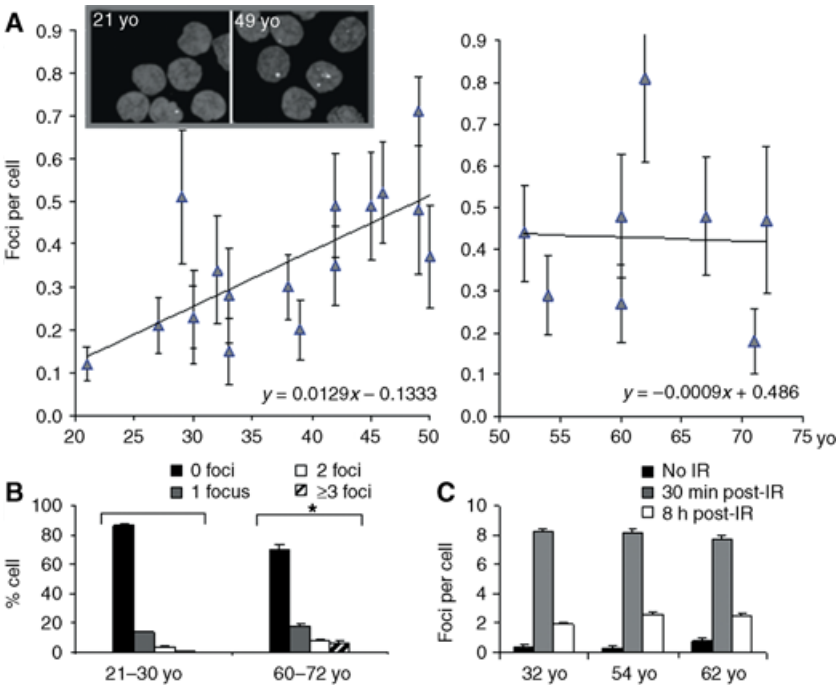

Fig. 1 Detection of phosphorylated histone H2AX (γ-H2AX) foci in human lymphocytes. (A) Incidence of γ-H2AX foci per cell increases with donor age. The foci were counted in 100–200 cells. Representative images of γ-H2AX foci in lymphocytes from two donors of different ages are shown in the insert. (B) Proportion of cells containing multiple γ-H2AX foci is greater in older donor population; * denotes statistically significant difference in a group of older donors compared to the younger ones ($P < 0.01$). (C) Incidence of γ-H2AX foci in response to ionizing radiation (IR) is age independent as is the long-term dynamics of their post-IR disappearance. (A & C) Error bars signify standard errors; (B) error bars signify standard deviations; *n* (number of donors) = 5.

(Redon *et al*., 2002; Pilch *et al*., 2003; Sedelnikova *et al*., 2003), accumulate in senescent human cells (D'Adda di Fagagna *et al*., 2003; Bakkenist *et al*., 2004; Sedelnikova *et al*., 2004) as well as in germ and somatic cells of aged mice (Sedelnikova *et al*., 2004). Such foci were also detected in dermal fibroblasts from aged primates (Herbig *et al*., 2006; Jeyapalan *et al*., 2007). In contrast to foci formed in response to known causes, such as ionizing radiation (IR), these age-associated foci were proposed to contain unrepairable DSBs, which may have a causal role in aging (Sedelnikova *et al*., 2004).

Despite the mentioned *in vitro* and *in vivo* evidence for a link between accumulated DSBs and aging phenotypes in mammals, the molecular basis for the age-related accumulation of DSBs is poorly understood. To gain insight into age-dependent changes in DSB repair, we examined the formation of γ-H2AX foci as a very early event in DSB repair, the growth rate of these γ-H2AX foci and the dynamics of recruitment of the other DSB repair proteins. Our analyses of human cells from young versus old donors, same cell strains at low versus high population doublings (PDs) in culture and cells from normal donors versus WS patients highlight an aging-dependent change in the kinetics of DSB repair, which is common between *in vitro* and *in vivo* aging, as well as between normal and pathological aging.

Results

γ-H2AX foci accumulate with donor age

To investigate whether organismal age affects individual cells by modulating their response to DNA damage, we used γ-H2AX antibody staining to identify and quantify DNA DSBs in human lymphocytes and primary fibroblasts from healthy donors of different ages, as well as in primary fibroblasts from WS patients of different ages. Fresh peripheral blood lymphocytes taken from 26 normal donors aged 21–72 years generally exhibited an increased incidence of γ-H2AX foci in older individuals (Fig. 1A). The proportion of cells containing γ-H2AX foci is higher in older individuals, and there is a marked increase in the total number of cells with multiple foci (Fig. 1B). When lymphocytes from donors of different ages were exposed to 0.6 Gy IR, the number of IR-induced γ-H2AX foci present at 30 min post-IR was independent of donor age as was the long-term decrease in their numbers (Fig. 1C).

To determine if other cells exhibited characteristics similar to lymphocytes, we obtained primary fibroblasts from normal donors aged 35, 49 and 61 years, and from donors aged 25, 30 and 60 years with WS. Fibroblasts from older normal donors were found to exhibit greater incidences of γ-H2AX foci than those from younger donors, and those from WS donors exhibited greater focal incidences than those from normal donors (Supplementary Fig. S1A). In addition, fibroblast cultures also exhibited greater focal incidences with increased PDs and progress toward senescence [measured by increased fraction of senescence-associated β-galactosidase (SA β-gal) positive cells] in culture (Supplementary Fig. S1B). These data are more clearly shown in Fig. 2(A) with donor age increasing along the *X*-axis, average numbers of γ-H2AX foci per cell increasing along the *Y*-axis and PDs increasing along the *Z*-axis, as well as in Fig. 2(B). Focal incidences in normal human fibroblast (NHF) cultures derived from a newborn's foreskin [0 years old (yo)] and WI-38 fetal lung fibroblasts were presented in our earlier report (Sedelnikova *et al*., 2004), and served as control values in this

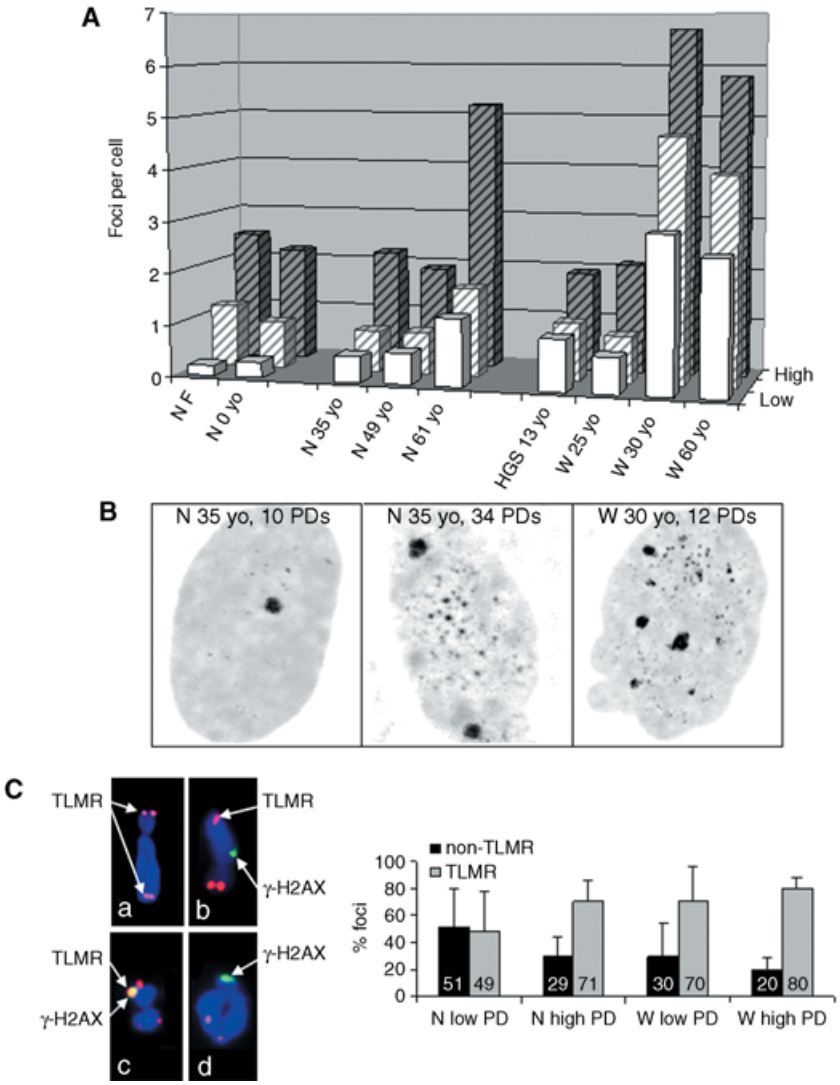

Fig. 2 Accumulation of phosphorylated histone H2AX (γ-H2AX) foci in primary fibroblasts from healthy (N) and Werner syndrome (WS) (W) donors. (A) In both normal and WS cells, the numbers of γ-H2AX foci increase with donor age and with progression toward replicative senescence. White, light striped and dark striped columns indicate low, intemediate and high population doublings (PDs), respectively. NF, normal fetus, WI-38 fibroblasts; N 0 years old (yo), normal human fibroblasts from a newborn; HGS, fibroblasts from an HGS donor. γ-H2AX foci were counted in 100–200 cells. More detailed analyses of each cell population along with representative cell images are shown in Supplementary Fig. S1, lower right corner. (B) Representative images compare low (10) and high (34) PD fibroblasts derived from a normal donor with low (12) PD fibroblasts from a WS donor of similar age (35 and 30 yo, respectively). Low PD WS cells exhibit a higher incidence of γ-H2AX foci (3 ± 0.9) compared to normal fibroblasts of both low PDs (0.5 ± 0.1) and high PDs (2.2 ± 0.4). The images also illustrate the appearance of a background 'noise'; small and bright multiple foci located throughout the nuclei in normal senescent cells and WS cells. (C) Endogenous γ-H2AX foci are both telomeric and non-telomeric. Left panel, representative chromosomes with γ-H2AX signal (green) and/or telomeric (TLMR) DNA probe (red): a, chromosome contains only telomere signals; b, γ-H2AX focus is localized along chromatid length and classified as non-telomeric; c, γ-H2AX focus is localized at chromatid end, co-localized with telomere signal (merged image is yellow) and classified as telomeric; d, γ-H2AX focus is localized at chromosomal end and classified as telomeric, although telomere signal is absent because of telomere shortening. Right panel, distribution of γ-H2AX foci in low and high PD cells from a healthy and a WS donor. The proportions of telomeric and non-telomeric γ-H2AX foci are shown and change during cellular senescence with increase of the telomeric fraction. The fraction of telomeric γ-H2AX foci is higher in WS cells than in normal cells. Error bars signify standard deviations; *n* (number of metaphases analyzed) = 11–18.

study. Although our conclusions are based on a limited number of available primary cell strains, and the human population is quite variable (as can be seen in Fig. 1A), these findings indicate that in addition to the positive correlation of γ-H2AX focal numbers with PDs in culture previously reported, there are similar positive correlations with donor age in normal fibroblasts and with WS fibroblasts. The higher frequencies of γ-H2AX foci correlated with higher total γ-H2AX levels, as measured by immunoblotting and by laser scanning cytometry (data not shown).

A procedure that combines γ-H2AX immunostaining and telomere fluorescence *in situ* hybridization (FISH) in interphase cells cannot properly distinguish between telomere-associated and telomere-independent age-related DNA damage (Sedelnikova *et al.*, 2004; Ksiazek *et al.*, 2007), because a telomere signal can

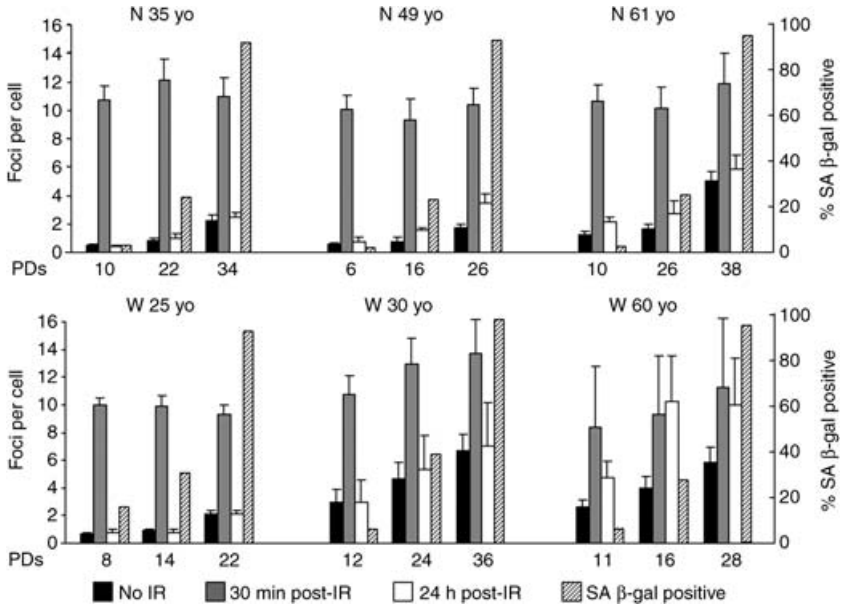

Fig. 3 Incidence of ionizing radiation (IR)-induced phosphorylated histone H2AX (γ-H2AX) foci and their long-term repair are independent of donor age and population doublings (PDs) in normal and Werner syndrome (WS) fibroblasts. Bars represent γ-H2AX foci per cell in primary cultures under three experimental conditions (unirradiated control, black bars; 30 min post-IR, gray bars, and 24 h post-IR, white bars). Striped bars correspond to senescence-associated β-galactosidase (SA β-gal) fractions. N, normal donors with age noted; W, WS donors with age noted. Error bars signify standard errors. With the exception of the 60-year-old (yo) WS donor, the incidence of γ-H2AX foci 24 h post-IR in these cell populations is similar to the pre-IR incidence, suggesting that long-term repair is not impaired.

be too short to be visualized. When this technique is applied to metaphase chromosomes, however (Nakamura *et al*., 2006), the precise location of γ-H2AX foci on the chromosomes can be determined and classified (Fig. 2C), including those at the chromosomal ends lacking a telomere repeat (Fig. 2C, d). Using this technique, we found that both telomeric and non-telomeric DNA damages are important determinants of mammalian senescence; however, mostly telomeric DNA damage accumulates during senescence in human cells (A. Nakamura, unpublished data). Here, we compared proportions of telomeric and non-telomeric γ-H2AX foci in young (low PD) and senescent (high PD) normal and WS fibroblasts (Fig. 2C). The fractions of telomere-associated γ-H2AX foci increased when both normal and WS cells progressed toward senescence, as well as in WS cells compared to normal cultures. These data suggest that increasing telomere dysfunction plays a primary role in producing senescence- and age-associated DNA damage in humans.

Next, we examined primary fibroblasts derived from normal and WS donors for their abilities to respond to IR (Fig. 3). The striped bars show the percentages of SA β-gal positive cells, which indicate a senescent state of cultures in each PD examined. A dose of 0.6 Gy induced comparable levels of γ-H2AX foci in all samples regardless of the origin, age or PDs (Fig. 3, gray bars). After 24 h, the incidences of IR-induced γ-H2AX foci had returned to values close to the numbers of γ-H2AX foci present in the unirradiated cells (Fig. 3, white bars) with the exception of the fibroblasts derived from a 60 yo WS patient, in which at middle and high PDs, the IR-induced γ-H2AX foci remained at 24 h, indicating a lack of DNA DSB repair in these cells.

Thus, two different cell types, quiescent lymphocytes and proliferating fibroblasts, both exhibit age-related increases in the incidence of γ-H2AX foci, although they are still competent in IR-induced DSB repair.

In addition to the large γ-H2AX foci counted for these studies, the fibroblasts from adult donors contained multiple smaller γ-H2AX spots which were of lower intensity than the large foci. The spots localized throughout the nuclei, mostly in low-propidium-iodide staining areas. A similar observation was previously described (McManus & Hendzel, 2005). These spots were much more pronounced in senescent cells (34 PD) from normal individuals (Fig. 2B, middle panel), but were found even in young (12 PD) WS cells (Fig. 2B, right panel). When the cells were co-stained with antibodies to MRN components, they co-localized only partially with these spots (data not shown), suggesting that these spots may not mark DNA DSBs. Therefore, although multiple small endogenous γ-H2AX-stained spots appear to be characteristic of aging cells, they are different from the aging-associated large DNA damage foci of interest in this study.

Kinetics of γ-H2AX focal growth and repair protein accumulation to γ-H2AX foci

The repair of DSBs involves fast and slow kinetic components. The analysis of real-time recruitment of DSB repair factors to sites of DNA damage in live cells revealed their accumulation on these sites immediately after generation of the damage (Lukas *et al*., 2004; Kruhlak *et al*., 2006a). Cells from H2AX-null mice, which lack the fast component of DSB repair, but fix DNA damage by 4 h post-IR, exhibit genomic instability and fail to accumulate repair proteins at DSB sites (Celeste *et al*., 2002, 2003a). The fast component of DSB rejoining may depend on the rapid formation of γ-H2AX foci which generally is completed by 15 min post-IR. To determine if WS cells, which exhibit genomic instability, also are deficient in the formation of γ-H2AX foci, we compared the initial kinetics of the focal formation and

recruitment of DSB repair proteins to these foci in normal and WS fibroblasts. In low PD NHFs, γ-H2AX foci enlarge rapidly reaching maximal size by 10 min post-IR (Fig. 4A, left montage; red arrows in the lower left panel indicate large γ-H2AX foci). Using double-labeling and separate-channel recording, we visualized the repair protein Mre11 accumulating at these γ-H2AX foci soon after they form (Fig. 4A; yellow foci in merged panels denote co-localization of γ-H2AX and Mre11 at 2 min post-IR; white arrows point to γ-H2AX foci deficient in Mre11). In contrast, high PD, senescent NHFs exhibit both slower enlargement of γ-H2AX foci and slower recruitment of Mre11 to these foci (Fig. 4A, right montage). The γ-H2AX foci in the high PD NHFs are noticeably smaller than those in the young NHFs at 10 min post-IR, and reach a size similar to those in the young NHFs only at 30–40 min post-IR (Fig. 4A, right montage; red arrows in the lower left panel indicate large γ-H2AX foci). In addition, Mre11 accumulates more slowly at the γ-H2AX foci, with many foci deficient in Mre11 at 10 and 30 min post-IR (Fig. 4A, right montage, merged panels; white arrows point to γ-H2AX foci deficient in Mre11). Similar accumulation kinetics was observed with Rad50 (data not shown). Line profiles of red (γ-H2AX) and green (Mre11) staining comparing low PD and high PD NHFs at 10 min post-IR (Fig. 4B) present a co-localization pattern for young cells and a lack of this pattern for senescent cells, supporting microscopy data. The delay of post-IR γ-H2AX focal growth in high PD cells correlates with a delayed increase of total γ-H2AX protein level in high PD NHFs, quantified by immunoblotting analysis (Fig. 4C). When the kinetics of γ-H2AX and Mre11 co-localization is quantified by computing pixel overlap [% of red pixels (γ-H2AX) coinciding spatially with green pixels (Mre11)], the large differences in Mre11 recruitment between low PD and high PD NHFs are readily apparent (Supplementary Fig. S2A). Particularly notable is the almost complete co-localization of γ-H2AX and Mre11 in the low PD NHFs and the lack of co-localization in the high PD, senescent NHFs at 10 min post-IR.

Next, WS fibroblasts were compared with NHFs for the rates of γ-H2AX focal enlargement and the mobilization of 53BP1, Mre11 and Rad50 proteins to IR-induced γ-H2AX foci (Fig. 5A,B). 53BP1 is recruited to γ-H2AX foci as soon as they form in the low PD NHFs (Fig. 4D, left montage), with few if any γ-H2AX foci deficient in 53BP1 content in the high PD, senescent NHFs (Fig. 4D, right montage). In contrast, in the low PD WS cells, a considerable number of γ-H2AX foci appear to be deficient in 53BP1 at 10 min post-IR, and a few still at 30 min post-IR (Fig. 5A, left montage; red spots in merged images). In the high PD, senescent WS cells, many γ-H2AX foci are deficient in 53BP1 at 30 min post-IR, and a few at 60 min post-IR (Fig. 5A, right montage; red spots in merged images). The kinetics of γ-H2AX and 53BP1 co-localization quantified by pixel overlap for NHFs and WS cells is presented in Supplementary Fig. S2(B). The data are consistent with the slower growth of the γ-H2AX foci in WS cells. In contrast to NHFs where the foci appear immediately after IR exposure, focal formation in the low PD WS cells begins 10 min post-IR, and in the high PD, senescent cells 30 min post-IR (Fig. 5A, left and right montages; red arrows). Thus, a substantial delay in the growth of γ-H2AX foci was coincident with delayed recruitment of DSB repair proteins.

The contrast between normal and WS cells is even more dramatic in the recruitment of Mre11 and Rad50. While these two repair proteins are co-localized with γ-H2AX foci soon after IR exposure in the low PD NHFs, in the low PD WS cells, considerable numbers of γ-H2AX foci are deficient in these proteins at 4 and 8 h post-IR (Fig. 5B, left and right montages; white arrows), and even at 20 h in the senescent WS cells (images not shown). The kinetics of γ-H2AX and Mre11 co-localization quantified by pixel overlap for two pairs of age-matching normal and WS cells is presented in Supplementary Fig. S2(C),(D).

The results of the time course experiment which measured the post-IR time required for maximum co-localization of Mre11 to IR-induced γ-H2AX foci (no more foci co-localized after these time points) in low and high PD primary cells from normal donors and WS donors of different ages, are summarized in Fig. 5(C) (Rad50 is similar; not shown). Normal fibroblasts at low PDs exhibit markedly increased time of recruitment of the repair proteins to γ-H2AX foci with increased age of the donor. While NHFs from a newborn, as well as fetal WI-38 cultures, exhibit a co-localization pattern by 10 min post-IR, those from 35 yo, 49 yo and 61 yo donors require 0.5 h, 1 h and 4 h, respectively. Low PD WS fibroblasts from 25 yo, 30 yo and 60 yo donors required 4 h or 8 h to complete the task. A delay in the maximal co-localization of the proteins was always observed in senescent cells. Markedly, in senescent fibroblasts from a 60 yo WS patient in which IR-induced γ-H2AX foci did not decrease 24 h post-exposure (see Fig. 2), Rad50 and Mre11 failed to accumulate at the sites of γ-H2AX foci ('∞' in Fig. 5C and red circles in Supplementary Fig. S2D).

One cell strain listed as WS (AG04110, 13 yo woman) was later discovered to be Hutchinson–Gilford progeria (*HGS*, *LMNA* gene mutation). Interestingly, γ-H2AX focal incidence was significantly elevated in the low PD *HGS* fibroblasts compared to the low PD NHFs (1 ± 0.3 foci per cell vs. 0.3 ± 0.1 foci per cell, respectively; Supplementary Figs S1 and S2A), and Rad50 and Mre11 proteins accumulated at the γ-H2AX foci only after 4 h post-IR, showing a kinetics similar to the WS cells (Fig. 5C). These data suggest a common mechanism for impaired DNA repair in prematurely aged cells with genomic instability.

Discussion

Accumulation of damage to macromolecules is thought to be one of the major causes of aging and age-related diseases. A DNA DSB is a molecular event with profound and often deleterious consequences for the genome and for the cell because it may cause loss of genetic information, affect chromosome separation during mitosis, influence replication fork progression, or when improperly repaired, cause chromosome rearrangements, cellular senescence or activation of apoptotic pathways. It is therefore no surprise that several studies in the past few years pointed to the significance of accumulation of DNA DSBs and the efficiency of their repair in cellular senescence and organismal

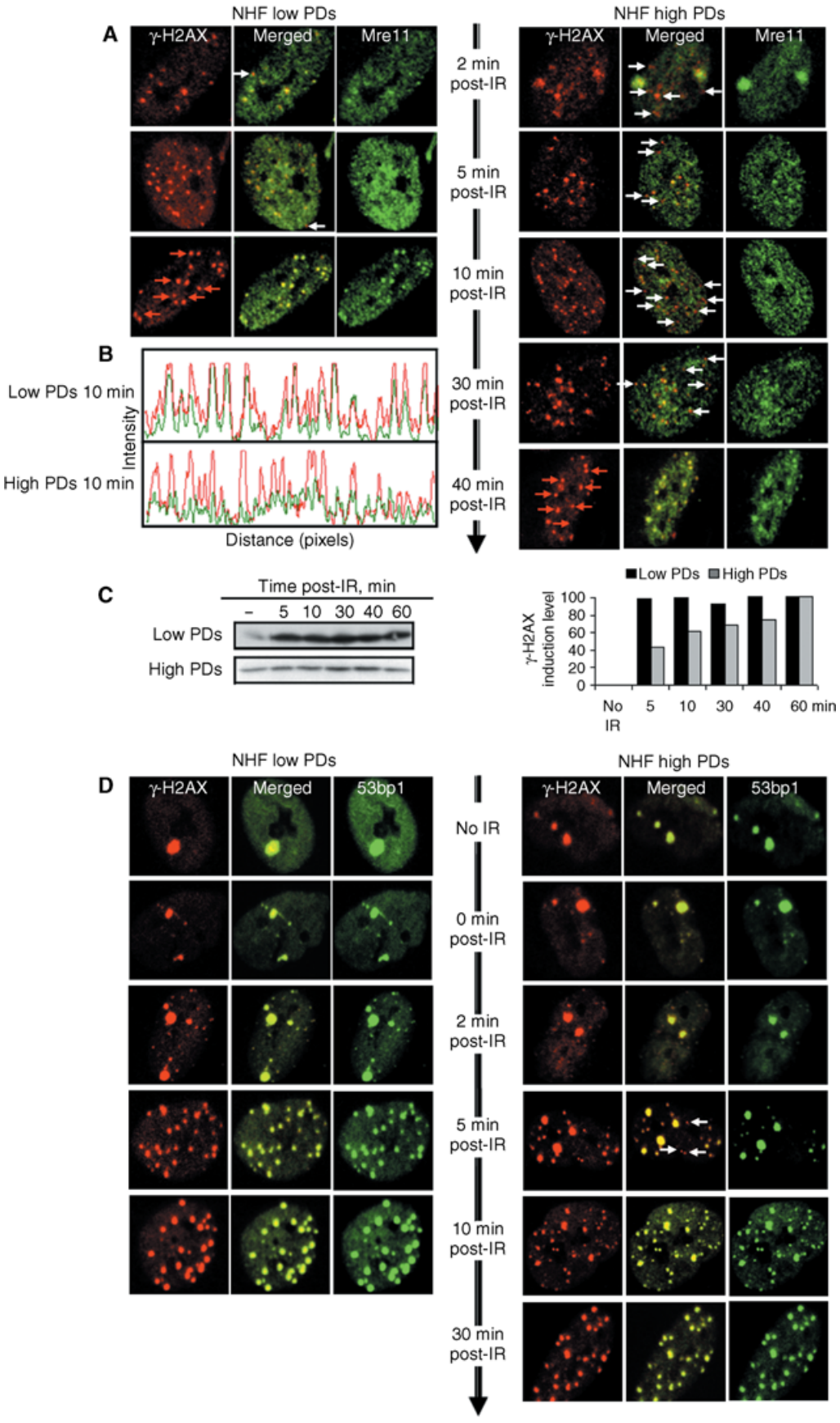

aging (D'Adda di Fagagna *et al*., 2003; Sedelnikova *et al*., 2004; Herbig *et al*., 2006; Jeyapalan *et al*., 2007; Nijnik *et al*., 2007; Rossi *et al*., 2007). To gain insight into the mechanisms underlying age-impaired DSB repair, we examined how endogenous levels of DNA damage, rates of short- and long-term IR-induced damage repair, γ-H2AX focal growth and accumulation of DSB repair proteins depend on human age.

Although cellular senescence and organismal aging share similar patterns, the relationship between the two remains an open question. Presented data obtained on human lymphocytes and fibroblasts from healthy donors of different ages show a two-directional increase in the number of γ-H2AX foci relative to both the age of donor and to PDs in culture. These observations confirm and expand our previous findings (Sedelnikova *et al*., 2004) that incidence of γ-H2AX foci increases similarly in mouse tissues during aging, and in human cells during senescence. Our data also demonstrate higher retention of damage in samples from older individuals, which may be a reflection of age-related decline in both the DNA DSB repair efficiency and fidelity (Mayer *et al*., 1991; Gorbunova & Seluanov, 2005; Hazane *et al*., 2006). It is noteworthy that cells derived from patients with WS, exhibited similar patterns of γ-H2AX focal accumulation, albeit the amplitudes were higher and the increases were detectable at a younger age. WRN protein prevents DNA breaks following alteration in chromatin topology (Turaga *et al*., 2007); knockdown of WRN or BLM proteins has been shown to induce increased incidences of γ-H2AX foci, compared to complemented cells (Szekely *et al*., 2005; Rao *et al*., 2007), similar to tumor cell lines (Sedelnikova & Bonner, 2006).

Our previous study of γ-H2AX foci and associated repair proteins in primary human fibroblasts (Sedelnikova *et al*., 2004) indicated the existence of two types of γ-H2AX foci, transient, where successful DSB repair occurs, and persistent, containing unrepairable DSBs, with a tendency to accumulate in senescing cells and in cells derived from aging subjects. In this study, we expanded upon that observation and showed, using a co-localization approach, that after IR, the rate of recruitment of repair proteins to the sites of γ-H2AX foci was substantially lower in NHF cells at advanced PDs compared to those from lower ones. The speed of recruitment of repair proteins was also attenuated relative to donor age – the older the donor, the slower the assembly of repair machinery at the sites of γ-H2AX foci. Therefore, cells approaching senescence and cells from aging donors are characterized by slower DNA DSB repair and, consequently, by accumulation of persistent DNA lesions. From our findings, we hypothesize that genome functional integrity may depend on the rapid formation and enlargement of damage-induced γ-H2AX foci and on the rapid accumulation of DSB repair proteins at these foci. In that respect, the slowed mobilization of repair proteins can be because of their decreased expression, a process associated with aging (Ju *et al*., 2006; Seluanov *et al*., 2007).

We found that WS cells exhibited a dramatically long delay in repair protein recruitment. A possible explanation may be the fact that RecQ helicases, one of which is the protein coded by the *WRN* gene, were shown (Otterlei *et al*., 2006; Kusumoto *et al*., 2007) to interact with other molecular factors involved in homologous recombination, which is one mechanism of DNA DSB repair. We are tempted to speculate that the absence of WRN protein might impair the recruitment dynamics of other factors involved, despite undisturbed γ-H2AX signaling. The WS phenotype appears also to be linked to telomere status, which, in turn, has been associated with γ-H2AX focal formation (Eller *et al*., 2006). Induced expression of telomerase reverses premature senescence in WS cells. Additionally, WRN-null mice do not exhibit premature aging (Crabbe *et al*., 2007). However, telomerase-null, WRN-null mice do exhibit the characteristics of WS after several generations, that is, when telomere lengths have become critically short (Chang *et al*., 2004; Chiang *et al*., 2004). Here, we show that WS cells have more telomere-associated DNA damage compared to normal cells. It may therefore be also possible that slower DSB repair protein accumulation in WS cells is a result of critically short telomeres.

The generation and analysis of H2AX-deficient mice demonstrated that H2AX is an active component of DNA damage response. These mice lack the fast element of DNA repair and exhibit genomic instability; the loss of just one H2AX allele compromises genomic integrity (Celeste *et al*., 2002, 2003b). Although the migration of repair and signaling proteins to DSBs is not abrogated in H2AX-null cells, they fail to form IR-induced foci. Therefore, γ-H2AX functions to concentrate proteins in the vicinity of DNA lesions, amplifying the signals that might be important at threshold levels of DNA damage (Celeste *et al*., 2003a; Fernandez-Capetillo *et al*., 2003). Also, H2AX phosphorylation may induce structural changes in chromatin, which are necessary during different stages of the DNA damage response (Kruhlak *et al*., 2006a,b), and the size and distribution of γ-H2AX foci within nuclear volume may provide a platform for

Fig. 4 High population doubling (PD) normal human fibroblasts (NHFs) exhibit slower phosphorylated histone H2AX (γ-H2AX) focal enlargement and of repair protein mobilization to the sites of ionizing radiation (IR)-induced γ-H2AX foci than do low PD NHFs. Red (γ-H2AX) and green (Mre11 or 53BP1) fluorochromes appear yellow where they coincide in the merged images. (A) Representative images of low (38) and high (68, senescent) PD NHFs stained for γ-H2AX and Mre11 at various times post-IR. Red arrows in lower left images point to γ-H2AX foci of similar size at 10 min post-IR in low PD cells, and at 40 min in high PD, senescent cells. White arrows in merged panels point to γ-H2AX foci deficient in Mre11. In low PD cells, the two proteins completely co-localized by 10 min post-IR, but the process required 40 min in high PD cells. (B) Line profiles of low and high PD NHFs at 10 min post-IR confirm visual presentation. For low PD NHFs, most of red (γ-H2AX profile) and green (Mre11 profile) lines coincide, while high PD NHFs lack the co-localization pattern at this particular time point. (C) Post-IR increase of total γ-H2AX protein follows different kinetics in low and high PD NHFs. Left panel, γ-H2AX levels after 5 Gy irradiation in young and senescent NHFs. Right panel, relative induction of γ-H2AX in irradiated NHFs versus unirradiated cells (quantification of immunoblotting in the left panel). Maximal induction of γ-H2AX is delayed in senescent NHFs. The values were normalized to the total H2AX levels (not shown). (D) 53BP1 accumulation at γ-H2AX foci. Representative images of low and high PD NHFs stained for γ-H2AX and 53BP1 taken at various times post-IR. The rate of 53BP1 co-localization with γ-H2AX foci is slower in high PD, senescent cells compared to low PD NHFs (10 min vs. 0 min). White arrows point to γ-H2AX foci deficient in 53BP1.

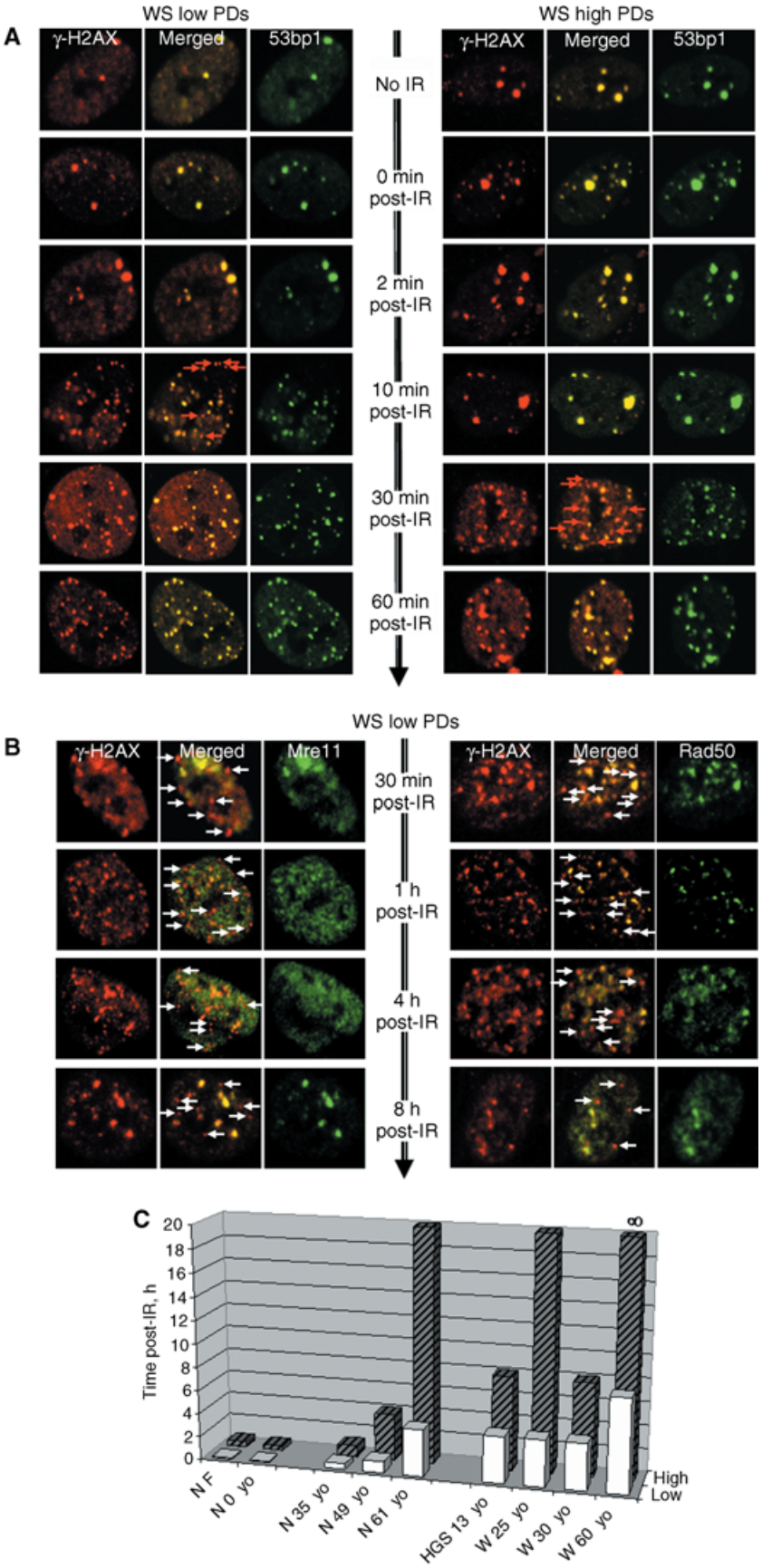

the immediate and robust response to DNA damage (Bewersdorf *et al*., 2006). These results indicate that fast DNA damage repair and accumulation of repair factors at DSBs are essential for an organism's well-being and genome maintenance. Xie *et al*. 2004 showed that repair was qualitatively different in H2AX-null mice, utilizing more short-patch single-strand annealing, an error-prone mechanism of DSB repair, in which information was deleted. Therefore, the hypothesis has been proposed that γ-H2AX 'shapes' the repair process in favor or error-free interchromatid homologous recombination. In the case of aging cells, slower formation of γ-H2AX foci and slower accumulation of repair proteins may shift the balance toward error-prone end joining and consequently accumulation of endogenous DNA damage.

Our study provides compelling evidence that accumulation of DNA damage and a reduced ability to repair such damage play an important role in physiological and pathological aging. Given the close association between aging and cancer development, the relevance of these observations has wider implications. We expect that our results will open a novel window to dissect early DSB repair processes, and will offer insights into the mechanisms of γ-H2AX focal growth and DNA repair protein accumulation. In this way, we can investigate how differences in these processes may lead to genome instability and defective phenotypes. The significance of this study is that it offers a strategy to elucidate the mechanism of rapid protein accumulation, and to measure how important the rate of protein accumulation at γ-H2AX foci is to the rapid component of DSB repair, genome stability and aging.

Experimental procedures

Human lymphocytes and cell cultures

Lymphocytes were isolated from whole blood obtained at the NIH blood bank in accordance with NIH regulations from 26 healthy donors aged 21–72 years. Five donors represented the youngest available population (21–30 yo), six donors represented the oldest available donor population (60–72 yo) and 15 donors were in the middle age group. To avoid stress-induced DNA damage post-isolation, the whole blood samples were processed for IR and/or fixation within 30 min post-blood draw.

Normal human fibroblasts derived from foreskin of a newborn were a gift from Dr Jayne Boyer (University of North Carolina). WI-38 fetal lung fibroblasts and normal primary fibroblasts derived from healthy adults of different ages (AG02603, lung, woman, 35 yo; AG02222, skin, man, 49 yo; AG02262, lung, man, 61 yo) were purchased from Coriell Cell Repositories (Camden, NJ, USA). From the same source came primary skin fibroblasts from WS patients (AG05229, man, 25 yo; AG03141, woman, 30 yo; AG00780 man, 60 yo) with confirmed mutation in *WRN* gene and a lack of WRN protein in Western blots. AG04110 skin fibroblasts (woman, 13 yo), with confirmed *LMNA* mutation, were also purchased from Coriell.

All fibroblast cultures were maintained at 37 °C, 5% CO_2, 20% oxygen according to recommended protocols. All cell strains were subcultured at a split ratio 1 : 4. The number of cells was counted in each passage, and the number of PDs achieved between passages was determined by $\log_2$ (number of cells obtained/number of cells inoculated) (Pereira-Smith & Smith, 1981; Sugawara *et al*., 1990). The largest PD for each cell strain was at, or very close to, complete senescence (when the cells stopped dividing and > 90% of the cells were SA β-gal positive), with no or very little cell proliferation (the BrdU incorporation rate was < 2%).

SA β-gal staining of intact cell cultures was performed with Senescence β-galactosidase staining kit (Cell Signalling, Beverly, MA, USA) according to the manufacturer's instructions (Dimri *et al*., 1995).

Immunocytochemistry and laser scanning confocal microscopy

For studies involving lymphocytes, 800 μL samples of anticoagulated whole blood were irradiated in a Mark I γ-irradiator (JL Shepherd & Associates, San Fernando, CA, USA) and fixed with 2% paraformaldehyde for 20 min at room temperature after different periods of incubation at 37 °C. Unirradiated blood samples were fixed the same way. After fixation, the samples were diluted 1 : 0.25 with phosphate-buffered saline (PBS) and layered directly onto 12 volumes of lymphocyte separation medium (Cambrex, Walkersville, MD, USA). Following centrifugation at 400 *g* for 30 min, the lymphocyte-containing interfaces were collected, washed twice with PBS and cytocentrifuged onto microscope slides. For immunofluorescence, PBS was replaced with PBS containing 0.5% Tween 20 and 0.1% Triton X-100 (Bio-Rad, Hercules, CA, USA) for blocking and antibody incubations. Staining was performed as previously described (Rogakou *et al*., 1999).

Fig. 5 Rates of phosphorylated histone H2AX (γ-H2AX) focal enlargement and mobilization of repair proteins in Werner syndrome (WS) cells. (A) 53BP1 accumulation. Representative images of low (12) and high (36) population doubling (PD) senescent WS cells stained for γ-H2AX (red) and 53BP1 (green) taken at various times post-ionizing radiation (IR). Coincident red and green signals appear yellow. Red arrows point to γ-H2AX foci that become visible at 10 min post-IR in low PD, and at 30 min post-IR in high PD senescent WS cells. γ-H2AX focal enlargement appears complete by 60 min, although a high homogeneous background (which disappears later) makes it more difficult to distinguish the foci, especially in high PD senescent cells. Complete 53BP1 co-localization with γ-H2AX foci is slower in WS cells than in normal human fibroblasts (NHFs) (see Fig. 4D), 30 min for low PD WS cells versus 0 min for low PD NHFs, and 60 min for high PD, senescent WS cells versus 10 min for high PD, senescent NHFs. (B) Mre11 and Rad50 accumulation in low PD WS cells. Representative images of low PD WS cells stained for γ-H2AX and either Mre11 (left montage) or Rad50 (right montage) taken at various times post-IR. Accumulation of Mre11 and Rad50 at γ-H2AX foci is incomplete even at 8 h post-IR in the WS cells compared to complete accumulation at 10 min in the NHFs (Fig. 4A, left montage). White arrows identify γ-H2AX foci deficient in 53BP1. (C) Time post-IR required for maximum co-localization of Mre11 with γ-H2AX in low and high PD, senescent fibroblasts from normal and WS donors of various ages. Data for fibroblasts from fetus (WI-38, NF), from newborn [N 0 years old (yo)], and from an HGS donor (HGS) are also shown. There is a positive correlation between donor age and the time for maximal repair protein accumulation to the sites of IR-induced double-strand breaks. High PD, senescent cells from a 60 yo WS donor exhibited incomplete co-localization at the longest time examined. White columns, low PD cells; dark striped columns, high PD cells.

For studies involving low, intermediate and high-PD fibroblast cultures, cells were initially plated on Labtek II slides (Nalge Nunc International, Naperville, IL, USA) at a density of 2×10^5 cells per well, and then irradiated, or intact cultures were further processed for fixation and immunostaining.

For short-time experiments, cells were exposed to γ-IR on ice. Warm media were added to the wells, and cultures were fixed at the noted times post-warm up. For double labeling, anti-γ-H2AX primary antibody was either from rabbit (custom made) or mouse (Upstate BioTech, Lake Placid, NY, USA) depending on the origin of the other antibodies, anti-Rad50, anti-Mre11 or anti-53BP1 (Novus Biologicals, Inc., Littleton, CO, USA). Alexa-488- or Alexa-555-conjugated IgG were obtained from Invitrogen (Eugene, OR, USA). Laser scanning confocal microscopy was performed with a Nikon PCM 2000 (Nikon, Inc, Augusta, GA, USA). The foci were visually counted in 100–200 cells. Quantification of red/green pixel ratios was performed with Image Pro 6.2 Analyzer software (Media Cybernetics, Bethesda, MD, USA); the values for each time point were quantified as averages of three to five microscopic fields.

Immunocytochemistry and FISH

Metaphase spreads were prepared as previously described (Nakamura *et al*., 2006). The slides were stained with mouse monoclonal anti-γ-H2AX antibody followed with Alexa-488-conjugated anti-mouse IgG. Staining for telomere FISH was performed according to telomere FISH kit (DakoCytomation, Glostrup, Denmark) protocol with some modifications. Briefly, γ-H2AX-stained cells were fixed with 50 mM ethylene glycol-*bis* (succinic acid *N*-hydroxy-succinimide ester) (Sigma, St. Louis, MO, USA), and then hybridization was performed according to the kit instructions. 4,6-Diamidino-2-phenylindole-dihydrochloride) was used for visualization of DNA. Fluorescent microscopy was performed with Olympus fluorescent microscope (Olympus America, Inc., Melville, NY, USA).

Western blot analysis

Normal human fibroblast cultures were irradiated with 5 Gy on ice, and then warm media were added and cells were collected at the noted times post-warm up. The cells were lysed in SDS Sample Buffer (Quality Biologicals, Inc., Gaithersburg, MD, USA). Cell extracts were electrophoresed in 4–20% Tris–glycine gels (Invitrogen, Carlsbad, CA) and transferred to polyvinylidene difluoride membranes (Invitrogen). The membranes were incubated with mouse anti-γ-H2AX and rabbit anti-H2AX antibodies (Upstate). Immunoreactive bands were visualized by using enhanced chemiluminescence (Western blotting detection reagents, Amersham Biosciences, Buckinghamshire, England).

Acknowledgments

We thank Scott Lawrence, SAIC, for developing Image Pro 6.2 Analyzer protein co-localization script, and Jennifer Dickey, NCI, for critical reading of the manuscript. This study was funded by the Intramural Research Program of the National Cancer Institute, Center for Cancer Research, NIH.

References

Bakkenist CJ, Drissi R., Wu J, Kastan MB, Dome JS (2004) Disappearance of the telomere dysfunction-induced stress response in fully senescent cells. *Cancer Res*. **64**, 3748–3752.

Bartkova J, Rezaei N, Liontos M, Karakaidos P, Kletsas D, Issaeva N, Vassiliou LV, Kolettas E, Niforou K, Zoumpourlis VC, Takaoka M, Nakagawa H, Tort F, Fugger K, Johansson F, Sehested M, Andersen CL, Dyrskjot L, Orntoft T, Lukas J, Kittas C, Helleday T, Halazonetis TD, Bartek J, Gorgoulis VG (2006) Oncogene-induced senescence is part of the tumorigenesis barrier imposed by DNA damage checkpoints. *Nature* **444**, 633–637.

Bewersdorf J, Bennett BT, Knight KL (2006) H2AX chromatin structures and their response to DNA damage revealed by 4Pi microscopy. *Proc. Natl. Acad. Sci. USA* **103**, 18137–18142.

Bohr VA (2005) Deficient DNA repair in the human progeroid disorder, Werner syndrome. *Mutat. Res*. **577**, 252–259.

Campisi J (2005) Senescent cells, tumor suppression, and organismal aging: good citizens, bad neighbors. *Cell* **120**, 513–522.

Celeste A, Petersen S, Romanienko PJ, Fernandez-Capetillo O, Chen HT, Sedelnikova OA, Reina-San-Martin B, Coppola V, Meffre E, Difilippantonio MJ, Redon C, Pilch DR, Olaru A, Eckhaus M, Camerini-Otero RD, Tessarollo L, Livak F, Manova K, Bonner WM, Nussenzweig MC, Nussenzweig A (2002) Genomic instability in mice lacking histone H2AX. *Science* **296**, 922–927.

Celeste A, Fernandez-Capetillo O, Kruhlak MJ, Pilch DR, Staudt DW, Lee A, Bonner RF, Bonner WM, Nussenzweig A (2003a) Histone H2AX phosphorylation is dispensable for the initial recognition of DNA breaks. *Nat. Cell Biol*. **5**, 675–679.

Celeste A, Difilippantonio S, Difilippantonio MJ, Fernandez-Capetillo O, Pilch DR, Sedelnikova OA, Eckhaus M, Ried T, Bonner WM, Nussenzweig A (2003b) H2AX haploinsufficiency modifies genomic stability and tumor susceptibility. *Cell* **114**, 371–383.

Chang S, Multani AS, Cabrera NG, Naylor ML, Laud P, Lombard D, Pathak S, Guarente L, DePinho RA (2004) Essential role of limiting telomeres in the pathogenesis of Werner syndrome. *Nat. Genet*. **36**, 877–882.

Cheng W-H, Muftuoglu M, Bohr VA (2007) Werner syndrome protein: functions in response to DNA damage and replication stress in S-phase. *Exp. Gerontol*. **42**, 871–878.

Chiang YJ, Hemann MT, Hathcock KS, Tessarollo L, Feigenbaum L, Hahn WC, Hodes RJ (2004) Expression of telomerase RNA template, but not telomerase reverse transcriptase, is limiting for telomere length maintenance *in vivo*. *Mol. Cell Biol*. **24**, 7024–7031.

Collado M, Blasco M, Serrano M (2007) Cellular senescence in cancer and aging. *Cell* **130**, 223–233.

Colavitti R, Finkel T (2005) Reactive oxygen species as mediators of cellular senescence. *IUBMB Life* **57**, 277–281.

Crabbe L, Jauch A, Naeger CM, Holtgreve-Grez H, Karlseder J (2007) Telomere dysfunction as a cause of genomic instability in Werner syndrome. *Proc. Natl. Acad. Sci. USA* **104**, 2205–2210.

D'Adda di Fagagna F, Reaper PM, Clay-Farrace L, Fiegler H, Carr P, Von Zglinicki T, Saretzki G, Carter NP, Jackson SP (2003) A DNA damage checkpoint response in telomere-initiated senescence. *Nature* **426**, 194–198.

De Boer J, Andressoo JO, de Wit J, Huijmans J, Beems RB, van Steeg H, Weeda G, van der Horst GT, van Leeuwen W, Themmen AP, Meradji M, Hoeijmakers JH (2002) Premature aging in mice deficient in DNA repair and transcription. *Science* **296**, 1276–1279.

Dhillon KK, Sidorova J, Saintigny Y, Poot M, Gollahon K, Rabinovitch PS, Monnat RJ Jr (2007) Functional role of the Werner syndrome RecQ helicase in human fibroblasts. *Aging Cell* **6**, 53–61.

Di Micco R, Fumagalli M, Cicalese A, Piccinin S, Gasparini P, Luise C, Schurra C, Garre' M, Nuciforo PG, Bensimon A, Maestro R., Pelicci PG, d'Adda di Fagagna F (2006) Oncogene-induced senescence is a DNA damage response triggered by DNA hyper-replication. *Nature* **444**, 638–642.

Dimri GP, Lee X, Basile G, Acosta M, Scott G, Roskelley C, Medrano EE, Linskens M, Rubelj I, Pereira-Smith O, Peacocke M, Campisi J (1995) A biomarker that identifies senescent human cells in culture and in aging skin *in vivo*. *Proc. Natl. Acad. Sci. USA* **92**, 9363–9367.

Eller MS, Liao X, Liu SY, Hanna K, Bäckvall H, Opresko PL, Bohr VA, Gilchrest BA (2006) A role for WRN in telomere-based DNA damage responses. *Proc. Natl. Acad. Sci. USA* **103**, 15073–15078.

Fernandez-Capetillo O, Celeste A, Nussenzweig A (2003) Focusing on foci. H2AX and the recruitment of DNA-damage response factors. *Cell Cycle* **2**, 426–427.

Gorbunova V, Seluanov A (2005) Making ends meet in old age: DSB repair and aging. *Mech. Ageing Dev*. **126**, 621–628.

Hasty P, Vijg J (2002) Aging. Genomic priorities in aging. *Science* **296**, 1250–1251.

Hasty P, Campisi J, Hoeijmakers J, van Steeg H, Vijg J (2003) Aging and genome maintenance: lessons from the mouse? *Science* **299**, 1355–1359.

Hazane FS, Sauvaigo Douki T, Favier A, Beani JC (2006) Age-dependent DNA repair and cell cycle distribution of human skin fibroblasts in response to UVA irradiation. *J. Photochem. Photobiol. B, Biol*. **82**, 214–223.

Herbig U, Ferreira M, Condel L, Carey D, Sadivy JM (2006) Cellular senescence in aging primates. *Science* **311**, 1257.

Hickson ID (2003) RecQ helicases: caretakers of the genome. *Nat. Rev. Cancer* **3**, 169–178.

Jeyapalan JC, Ferreira M, Sedivy JM, Herbig U (2007) Accumulation of senescent cells in mitotic tissue of aging primates. *Mech. Ageing Dev*. **128**, 36–44.

Ju YJ, Lee KH, Park JE, Yi YS, Yun MY, Ham YH, Kim TJ, Choi HM, Han GJ, Lee JH, Lee J, Han JS, Lee KM, Park GH (2006) Decreased expression of DNA repair proteins Ku70 and Mre11 is associated with aging and may contribute to the cellular senescence. *Exp. Mol. Med*. **38**, 6868–6893.

Karanjawala ZE, Lieber MR (2004) DNA damage and aging. *Mech. Ageing Dev*. **125**, 405–416.

Kipling D, Davis T, Ostler EL, Faragher RG (2004) What can progeroid syndromes tell us about human aging? *Science* **305**, 1426–1431.

Kruhlak MJ, Celeste A, Dallaire G, Fernandez-Capetillo O, Muller WG, McNally JG, Bazett-Jones DP, Nussenzweig A (2006a) Changes in chromatin structure and mobility in living cells at sites of DNA double-strand breaks. *J. Cell Biol*. **172**, 823–834.

Kruhlak MJ, Celeste A, Nussenzweig A (2006b) Spatio-temporal dynamics of chromatin containing DNA breaks. *Cell Cycle* **5**, 1910–1912.

Ksiazek K, Passos JF, Olijslagers S, Saretzki G, Martin-Ruiz C, von Zglinicki T (2007) Premature senescence of mesothelial cells is associated with non-telomeric DNA damage. *Biochem. Biophys. Res. Commun*. **362**, 707–711.

Kusumoto R, Muftuoglu M, Bohr VA (2007) The role of WRN in DNA repair is affected by post-translational modifications. *Mech. Ageing Dev*. **128**, 50–57.

Kyng KJ, Bohr VA (2005) Gene expression and DNA repair in progeroid syndromes and human aging. *Ageing Res. Rev*. **4**, 579–602.

Liu Y, Rusinol A, Sinensky M, Wang Y, Zou Y (2006) DNA damage responses in progeroid syndromes arise from defective maturation of prelamin A. *J. Cell Sci*. **119**, 4644–4649.

Lukas C, Melander F, Stucki M, Falck J, Bekker-Jensen S, Goldberg M, Lerenthal Y, Jackson SP, Bartek J, Lukas J (2004) Mdc1 couples DNA double-strand break recognition by Nbs1 with its H2AX-dependent chromatin retention. *EMBO J*. **23**, 2674–2683.

Mattout A, Dechat T, Adam SA, Goldman RD, Gruenbaum Y (2006) Nuclear lamins, diseases and aging. *Curr. Opin. Cell Biol*. **18**, 335–341.

Mayer PJCS, Lange Bradley MO, Nichols WW (1991) Gender differences in age-related decline in DNA double-strand break damage and repair in lymphocytes. *Ann. Hum. Biol*. **18**, 405–415.

McManus KJ, Hendzel MJ (2005) ATM-dependent DNA damage-independent mitotic phosphorylation of H2AX in normally growing mammalian cells. *Mol. Biol. Cell* **16**, 5013–5025.

Nakamura A, Sedelnikova OA, Redon C, Pilch DR, Sinogeeva NI, Shroff R., Lichten M, Bonner WM (2006) Techniques for gamma-H2AX detection. *Meth. Enzymol*. **409**, 236–250.

Nehlin JO, Skovgaard GL, Bohr VA (2000) The Werner syndrome; a model for the study of human aging. *Ann. NY Acad. Sci*. **908**, 167–179.

Nijnik A, Wodbine L, Marchetti C, Dawson S, Lambe T, Liu C, Rodriges NP, Crockford TL, Cabuy E, Vindigni A, Enver T, Bell JI, Slijepcevic P, Goodnow CC, Jeggo PA, Cornall RJ (2007) DNA repair is limiting for haematopoetic stem cells during ageing. *Nature* **447**, 686–690.

Ostler EL, Wallis CV, Sheerin AN, Faragher RGA (2002) A model for phenotypic presentation of Werner's syndrome. *Exp. Gerontol*. **37**, 285–292.

Otterlei M, Bruheim P, Ahn B, Bussen W, Karmakar P, Baynton K, Bohr VA (2006) Werner syndrome protein participates in a complex with RAD51, RAD54, RAD54B and ATR in response to ICL-induced replication arrest. *J. Cell Sci*. **119**, 5137–5146.

Pereira-Smith OM, Smith JR (1981) Expression of SV40 T antigen in finite life-span hybrids of normal and SV-40-transformed fibroblasts. *Somatic Cell Genet*. **7**, 411–421.

Pilch DR, Sedelnikova OA, Redon C, Celeste A, Nussenzweig A, Bonner WM (2003) Characteristics of γ-H2AX foci formation at DNA double-strand break sites. *Biochem. Cell Biol*. **81**, 123–129.

Rao VA, Conti C, Guirouilh-Barbat J, Nakamura A, Miao Z-H, Davies SL, Sacca B, Hickson ID, Bensimon A, Pommier Y (2007) Endogenous γ-H2AX-ATM-Chk2 checkpoint activation in Bloom's syndrome helicase–deficient cells is related to DNA replication arrested fork. *Mol. Cancer Res*. **5**, 713–724.

Redon C, Pilch D, Rogakou E, Sedelnikova O, Newrock K, Bonner W (2002) Histone H2A variants H2AX and H2AZ. *Curr. Opin. Genet. Dev*. **12**, 162–169.

Rogakou EP, Boon C, Redon C, Bonner WM (1999) Megabase chromatin domains involved in DNA double-strand breaks *in vivo*. *J. Cell Biol*. **146**, 905–915.

Rossi DJ, Bryder D, Seita J, Nussenzweig A, Hoeijmakers J, Weissman IL (2007) Defiiciencies in DNA damage repair limit the function of haematopoetic stem cells with age. *Nature* **447**, 725–729.

Scaffidi P, Misteli T (2006) Lamin A-dependent nuclear defects in human aging. *Science* **312**, 1059–1063.

Sedelnikova OA, Bonner WM (2006) γ-H2AX in cancer cells: a potential biomarker for cancer diagnostics, prediction and recurrence. *Cell Cycle* **5**, 2909–2913.

Sedelnikova OA, Pilch DR, Redon C, Bonner WM (2003) Involvement of H2AX in the DNA damage and repair response. *Cancer Biol. Ther*. **2**, 233–235.

Sedelnikova OA, Horikawa I, Zimonjic DB, Popescu NC, Bonner WM, Barrett JC (2004) Senescing human cells and ageing mice accumulate DNA lesions with unrepairable double-strand breaks. *Nat. Cell Biol*. **6**, 168–170.

Seluanov A, Danek J, Hause N, Gorbunova V (2007) Changes in the level and distribution of Ku proteins during cellular senescence. *DNA Repair* **6**, 1740–1748.

Shen JC, Loeb LA (2001) Unwinding the molecular basis of the Werner syndrome. *Mech. Ageing Dev.* **122**, 921–944.

Singh NP, Ogburn CE, Wolf NS, van Belle G, Martin GM (2001) DNA double-strand breaks in mouse kidney cells with age. *Biogerontology* **2**, 261–270.

Stewart SA, Weinberg RA (2006) Telomeres: cancer to human aging. *Annu. Rev. Cell Dev. Biol.* **22**, 531–557.

Sugawara O, Oshimura M, Koi M, Annab LA, Barrett JC (1990) Induction of cellular senescence in immortalized cells by human chromosome 1. *Science* **247**, 707–710.

Szekely AM, Bleichert F, Numann A, Van Komen S, Manasanch E, Ben Nasr A, Canaan A, Weissman SM (2005) Werner protein protects non-proliferating cells from oxidative DNA damage. *Mol. Cell Biol.* **25**, 10492–10506.

Turaga RVN, Massip L, Chavez A, Johnos FB, Lebel M (2007) Werner syndrome protein prevents DNA breaks upon chromatin structure alteration. *Aging Cell* **6**, 471–481.

Xie A, Puget N, Shim I, Odate S, Jarzyna I, Bassing CH, Alt FW, Scully R. (2004) Control of sister chromatid recombination by histone H2AX. *Mol. Cell* **16**, 1017–1025.

Zhang H (2007) Molecular signaling and genetic pathways of senescence: its role in tumorigenesis and aging. *J. Cell Physiol.* **210**, 567–574.

Supplementary material

The following supplementary material is available for this article:

Fig. S1 (A) Accumulation of phosphorylated histone H2AX (γ-H2AX) foci in primary human fibroblasts during senescence and aging. Representative single-cell images of low (top row), intermediate (middle row) and high (bottom row) population doubling (PD) cells derived from normal donors [35, 49 and 61 years old (yo)], Werner syndrome donors (25, 30 and 60 yo) and one HGS donor (13 yo). The number of γ-H2AX foci per cell is shown in the lower right corner, the PD number is shown in the upper right corner, the percentage of senescence-associated β-galactosidase (SA β-gal)-positive cells is shown in the upper left corner and the percentage of foci-free cells is shown in the lower left corner. Blue, DNA, propidium iodide; green, γ-H2AX. (B) Representative field images of SA β-gal staining for low, intermediate and high PDs.

Fig. S2 Quantitative image analysis of repair protein accumulation. The kinetics of Mre11 or 53BP1 (green fluorophore) overlap with phosphorylated histone H2AX (γ-H2AX) (red fluorophore) is slower in high population doubling (PD), senescent cells, as well as in cells from older and Werner syndrome (WS) donors. The values were normalized to 100% for the highest percentage of the pixel overlap. Error bars signify standard deviations; *n* (number of microscopic fields analyzed) = 3–5. (A) Mre11 overlap with γ-H2AX pixels. Mre11 accumulation to γ-H2AX sites is delayed about 30 min in high PD, senescent normal human fibroblasts (NHFs) compared to low PD cells. (B) 53BP1 overlap with γ-H2AX pixels. 53BP1 accumulation to γ-H2AX sites is delayed 5–10 min in high PD, senescent NHFs compared to the almost immediate co-localization in low PD cells. Werner syndrome cells show a dramatically decreased rate of mobilization. Compared to NHFs, 53BP1 accumulation to γ-H2AX sites exhibits from a 30 min delay in low PD WS cells, to an indefinite delay in high PD, senescent WS cells. (C and D) Kinetics of Mre11 and γ-H2AX pixels overlaps for fibroblasts from 35-year-old (yo) and 61 yo healthy donors compared to cells from age-matched WS donors. Overlap kinetics is slower for high PD, senescent cells versus low PD cells from all types of donors, as well as for cells from WS donors versus normal donors of similar age. Notice that the *X*-axis scale is different: 0–40 min for young/senescent NHFs, 0–8 h for 30 yo donors and 0–20 h for 60 yo donors. Cells from a 60 yo WS donor exhibit a completely retarded mobilization of Mre11.

This material is available as part of the online article from:
http://www.blackwell-synergy.com/doi/abs/10.1111/j.1474-9726.2007.00354.x
(This link will take you to the article abstract).

Please note: Blackwell Publishing are not responsible for the content or functionality of any supplementary materials supplied by the authors. Any queries (other than missing material) should be directed to the corresponding author for the article.